8-2014

Towards Zero-waste Mineral Carbon Sequestration Via Two-way Valorization of Ironmaking Slag

Yi Wai Chiang
Katholieke Universiteit Leuven

Rafael M. Santos
Katholieke Universiteit Leuven, rafael.santos@sheridancollege.ca

Jan Elsen
Katholieke Universiteit Leuven

Boudewijn Meesschaert
Katholieke Universiteit Leuven

Johan A. Martens
Katholieke Universiteit Leuven

Follow this and additional works at: https://source.sheridancollege.ca/fast_chem_publ

Part of the Chemical Engineering Commons

See next page for additional authors

SOURCE Citation

Authors

Yi Wai Chiang, Rafael M. Santos, Jan Elsen, Boudewijn Meesschaert, Johan A. Martens, and Tom Van Gerven

Accepted Manuscript

Towards zero-waste mineral carbon sequestration via two-way valorization of ironmaking slag

Yi Wai Chiang, Rafael M. Santos, Jan Elsen, Boudewijn Meesschaert, Johan A. Martens, Tom Van Gerven

Please cite this article as: Y.W. Chiang, R.M. Santos, J. Elsen, B. Meesschaert, J.A. Martens, T. Van Gerven, Towards zero-waste mineral carbon sequestration via two-way valorization of ironmaking slag, *Chemical Engineering Journal* (2014), doi: http://dx.doi.org/10.1016/j.cej.2014.03.104

Towards zero-waste mineral carbon sequestration via two-way valorization of ironmaking slag

Yi Wai Chiang [1,2,*], Rafael M. Santos [3], Jan Elsen [4], Boudewijn Meesschaert [1], Johan A. Martens [1], Tom Van Gerven [3]

[1] KU Leuven, Department of Microbial and Molecular Systems, Kasteelpark Arenberg 23, 3001 Leuven, Belgium.

[2] University of Guelph, School of Engineering, Albert A. Thornbrough Building, Guelph, Canada, N1G 2W1.

[3] KU Leuven, Department of Chemical Engineering, Willem de Croylaan 46, 3001 Leuven, Belgium.

[4] KU Leuven, Department of Earth and Environmental Sciences, Celestijnenlaan 200e, 3001 Leuven, Belgium.

*Corresponding author. Tel.: +1 519 824 4120, x58217.

Email addresses: chiange@uoguelph.ca (Y.W. Chiang); rafael.santos@alumni.utoronto.ca (R.M. Santos).

Abstract

A three-stage process was developed to transform blast furnace slag (BFS) into two valuable products: precipitated calcium carbonate (PCC) and zeolitic materials. The conceptualized process aims to simultaneously achieve sustainable CO_2 sequestration and solid waste elimination. Calcium is first selectively extracted by leaching with an organic acid, followed by carbonation of the leachate to precipitate $CaCO_3$. In parallel, the hydrothermal conversion of the extracted solid residues in alkali solution induces the dissolution/precipitation mechanism that leads to the formation of micro- and meso-porous zeolitic materials. Leaching selectivity was identified as a key factor in the valorization potential of both products. Acetic acid satisfactorily limited the leaching of aluminium, required for the subsequent synthesis of zeolites, and carbonation of the acetic acid leachate resulted in the production of PCC of varied mineralogy and morphology, depending on processing conditions. In the hydrothermal conversion stage, the formation of zeolitic phases was observed, and their characteristics were found to vary depending on the calcium extraction efficiency in the previous stage, and the alkali (NaOH) concentration. The zeolitic phases produced, in order of increasing valorization potential, were: tobermorite, sodalite, lazurite, and analcime.

1

Keywords: Mineral carbonation; Precipitated calcium carbonate; Hydrothermal conversion; Zeolitic materials; Blast furnace slag; Valorization.

1. Introduction

The utilization of waste materials such as steelmaking slags for CO_2 sequestration could be more appealing to the industry if the benefits of mineral carbonation and waste stabilization/valorization could be combined symbiotically. Indirect carbonation is especially interesting due to the production of high-purity products, particularly precipitated calcium carbonate (PCC) [1-6]; however, the generation of a large amount of destabilized solid residue (e.g. 0.73 t per tonne steel converter slag [5]), wherein hazardous heavy metal and metalloid components can become concentrated and mobilized [7], may hinder this approach. In order to meet the goal of sustainable CO_2 sequestration, a mineral carbonation processing scheme that results in zero solid waste is desirable. This study investigates the potential of two-way valorization of blast furnace slag (BFS), derived from carbon steel production, via: (i) production of PCC from the initial-stage extraction step; and (ii) utilization of the solid residue for the production of zeolitic materials via hydrothermal conversion.

Figure 1 presents a schematic flowsheet of the conceptualized process. Its principal advantage is the generation of two marketable products, which can potentially off-set the cost of carbon sequestration. In addition, the approach presents opportunities for process integration, such as that highlighted in Figure 1 (dashed line) whereby the residual alkalinity of the hydrothermal stage can be re-routed to the carbonation stage to induce carbonate precipitation. This integrated flowsheet can potentially contribute to the improvement of economic and environmental sustainability of mineral carbonation, thus advancing this route for carbon sequestration closer to industrial implementation.

Recent works on the production of PCC from steelmaking slags [3-6] have primarily focused on converter slag (also known as Basic Oxygen Furnace (BOF) slag), as this residue is in pressing need of new valorization routes [8]. However, this slag presents several inefficiencies as a carbon sink, which include: its relatively small production output compared to CO_2 emissions of steelworks; its monolithic morphology, requiring energy intensive milling to impart high reactivity; and its high intrinsic content of regulated heavy metals and metalloids [8]. In the

2

present study, blast furnace slag was chosen as the feedstock to the proposed process due to three factors: (i) its large and global production (0.25–0.30 t BFS per tonne crude iron, resulting in approximately 300 Mt BFS produced globally in 2011 [9]), allowing for meaningful carbon storage capacity; (ii) its rather consistent chemical and mineralogical composition compared to other residual materials, which have allowed it to be commercialized in stringent applications such as slag cements [10]; and (iii) its relatively high aluminum content (10–14 wt% Al_2O_3 [10]), an essential component of aluminosilicate-based zeolites [11]. BFS is currently valorized to a large extent in the cement industry for the production of blended cements where it partially replaces traditional Portland cement [10]. As the latter material has a large CO_2 footprint, due to calcination of limestone during production, this replacement results in reduction of CO_2 emissions. The present study aims to investigate an alternative and innovative valorization route that may result in higher value generation (PCC and zeolite) coupled to concomitant CO_2 abatement.

The production of PCC from steelmaking slags has been a major focus of research due to the numerous commercial applications for this material such as filler, pigment and colour stabilizer, paint extender, pH buffer and neutralizer, fertilizer and animal feed [12]. Of particular note are the works of Teir et al. [1] and Eloneva et al. [2], who used acetic acid (CH_3COOH) for the extraction of calcium from BFS, and later carbonated the leachate with the aid of sodium hydroxide (NaOH) as an acid neutralization agent, to precipitate calcium carbonate crystals. Based on these investigations, acetic was utilized as the leaching agent in the present study for the first-stage calcium leaching from BFS. The question pursued in the present study was if the use of acetic acid in the extraction stage allows the symbiotic balancing of PCC quality and zeolitic material utility, by delivering the necessary leaching extent and selectivity.

The hydrothermal conversion of silica- and alumina-rich solids into zeolitic minerals via heat treatment in highly alkaline solutions has been sought for the valorization of fly ashes and bottom ashes from coal combustion and waste incineration [11, 13]. The synthesis of zeolitic minerals from industrial and synthetic slags utilizing direct and indirect hydrothermal conversion methods has been reported by a limited number of researchers [14-16]. Sugano et al. [14] reported that when the CaO content of the raw material is higher than 20 wt% large quantities of undesirable phases form, due to their low microporosity; these include tobermorite ($Ca_5Si_6O_{16}(OH)_2 \cdot 4(H_2O)$) and hydrogarnet ($3CaO \cdot Al_2O_3 \cdot (3-x)SiO_2 \cdot 2xH_2O$, $0 \leq x \leq 3$). This

3

indicates that extensive removal of calcium is required in the extraction stage, which is in line with maximizing the output of PCC in the carbonation stage of the present conceptual process flowsheet.

Prior researches on the hydrothermal conversion of BFS did not, however, consider using extraction agents amiable to PCC production. Rather, Kuwahara et al. [15] applied concentrated hydrochloric acid (HCl) as the leaching agent, which, is not only impractical for mineral carbonation due to its high acid strength and energy intensive regeneration [16], also undesirably leached the majority of aluminum from the slag. Murakami et al. [17] applied formic acid (HCOOH) for selective leaching, finding that calcium and magnesium could be effectively removed after two extraction cycles at pH 2, while aluminum was left undisturbed. Hydrothermal conversion of the leached residue resulted in the formation of zeolite A ($Na_{12}(Al_{12}Si_{12}O_{48})\cdot 27H_2O$) and Na-P1 ($Na_6Al_6Si_6O_{32}\cdot 12H_2O$). The carbonation of calcium-containing formic acid leachates has not been comprehensively reported in literature. The fact that the acid dissociation constant of acetic acid is higher than that of formic acid (pKa of 4.76 and 3.75, respectively [18]) suggests that precipitation of calcium carbonate may be more readily achievable from acetate solutions. Thus, in the present work, the suitability of acetic leached BFS was investigated for the production of zeolitic materials, avoiding supplementary solid input materials (such as aluminum oxide) in order to maintain process simplicity and minimize production costs.

Furthermore, the aforementioned zeolites have been reported to possess affinity for heavy metal adsorption in water and wastewater treatment applications, and have also been applied as catalysts or catalyst supports [11, 13]. The production of such zeolitic materials from the leaching residues of indirect mineral carbonation thus represents an attractive valorization and waste minimization route. The aim of this study was to determine if leaching selectivity and extent obtained using acetic acid are satisfactory to enable synthesis of functional zeolitic products.

2. Materials and methods

2.1. Material characterization

The starting material was granulated blast furnace slag (GBFS) obtained from a steelworks. Prior to experimentation, the slag was milled using a centrifugal mill (Retsch ZM100) operated at 1400 rpm rotating speed and equipped with a 500 μm sieve mesh. The resulting material had a mean particle diameter (D[4,3]), determined by wet laser diffraction (LD, MalvernMastersizer S) of 138.3 μm.

The chemical composition was determined by wavelength dispersive X-ray fluorescence (WDXRF, Panalytical PW2400); the slag was found to contain mainly CaO (41.0 wt%), SiO_2 (36.0 wt%), Al_2O_3 (11.0 wt%) and MgO (8.4 wt%). Minor metallic components are Ti (0.50 wt%), Fe (0.22 wt%) and Mn (0.22 wt%). The main trace heavy metals detected are Ba (956±91 ppm), Sr (615±31 ppm) and V (160±32 ppm). Sulfur content is 1.1 wt%.

Mineralogical composition of GBFS was determined by X-ray diffraction (XRD, Philips PW1830 equipped with a graphite monochromator and a gas proportional detector, using Cu Kα radiation at 30 mA and 45 kV, step size of 0.03° 2θ and counting time of 2 s per step, over 5–70° 2θ range). The slag was found to be mainly amorphous, given the lack of defined diffraction peaks in its diffractogram and the observed broad pattern (Figure 2).

2.2. Experimental methodology

For the first-stage calcium extraction, analytical grade acetic acid was used as the leaching agent. To reduce acidity, which can have a detrimental effect on leaching selectivity, the extraction was done in two steps, using half the molar concentration otherwise required for one step. In each step, 731 ml acid solution (0.5–2.0 M) was mixed with the solids (100 g BFS in the first step) in a Büchi Ecoclave reactor (1.1 liter internal volume, electrically heated and water cooled, equipped with turbine impeller mixer). The slurry was mixed at 1000 rpm at 30 °C for 60 minutes in each step; these conditions were selected as optimal based on the work of Teir et al. [1]. To separate the leachate solution from the residual solids, the slurry was vacuum filtered using Whatman No. 2 filter paper. After the second extraction, the solids were filtered twice, the

5

second time with distilled water (DI) to wash out residual leachate solution from the filter cake. The residual solids were oven dried after the second extraction at 105 °C for 24 hours.

For the second-stage carbonation step, the extraction leachate was carbonated in the same Ecoclave reactor. Carbonation duration was fixed at 60 minutes, while temperature (90–120 °C) and CO_2 partial pressure (6–40 bar) were varied. Industrial quality (≥99.5%) CO_2 was used (Praxair). To buffer the acidity of the regenerated acetic acid upon carbonation and induce carbonate precipitation, one of two analytical grade additives was used in equimolar amounts relative to the acetate concentration of the leachates: sodium bicarbonate ($NaHCO_3$) or sodium hydroxide (NaOH). The carbonation precipitates were vacuum filtered from the slurry, washed thoroughly with DI water to remove soluble organic compounds, and dried in an oven at 105 °C for 24 hours.

In the parallel hydrothermal conversion stage, the residual solids from the first-stage extraction were mixed with 0.5–3 M NaOH solutions at a liquid-to-solids ratio (L/S) of 5 (18 g in 90 ml) in mechanically rotated autoclave bombs (internal volume 120 ml) for one to seven days at 150 °C. The final product was vacuum filtered from the slurry, washed thoroughly with DI water to remove excess caustic, and dried in an oven at 105 °C for 24 hours. After drying, hardened materials were milled using the centrifugal mill, while granular materials were manually disaggregated by mortar and pestle.

2.3. Analytical methods

Aqueous concentrations of Al, Ca, Mg and Si in the post-extraction leachates and post-carbonation filtered solutions were determined by inductively coupled plasma mass spectrometry (ICP-MS, Thermo Electron X Series). The mineralogical composition of solids recovered from the carbonation and hydrothermal conversion treatments was determined by Rietveld refinement [19] of XRD data using TOPAS Academic 4.1 (Coelho Software). The chemical composition of the produced solids was quantified by WDXRF and by energy dispersive X-ray spectroscopy (EDS, EDAX). Morphological features of the solid materials were visualized by scanning electron microscopy (SEM, Philips XL30 FEG). Microporous Brunauer–Emmett–Teller (BET) surface area of the hydrothermally converted solids was measured from nitrogen adsorption isotherm data collected in a Micromeritics TriStar 3000 analyzer.

3. Result and discussion

3.1. Extraction results

A comparison was made between the extraction efficiency and selectivity of different molarities of acetic acid, ranging from 0.5 to 2 M in each of two extraction steps. The lowest concentration results in a 2:1 calcium-to-acid molar ratio at each extraction step, or 1:1 in total. The purpose of using this concentration was to assess how close to stoichiometric the extraction extent is. The higher molarities were used once it was found that the extraction is not stoichiometric. The results of aluminum, calcium, magnesium and silicon extraction from milled GBFS are presented in Figure 3.

While the objective of the first-stage extraction is the leaching of calcium for the subsequent production of PCC, magnesium was also detected to assess the leaching selectivity, as magnesium is also an alkaline component that can be subjected to carbonation (although requiring more intensified conditions for precipitation than calcium [20]). As for aluminum, in view of producing aluminosilicate-based zeolitic sorbent minerals in the subsequent hydrothermal conversion stage, it is important for this element to remain in the solid phase. Lastly, the leaching of silicon was monitored as this is a major component of BFS and has the potential to contaminate the PCC product, thus degrading physical properties important for product commercialization (e.g. brightness [21]).

Figure 3 demonstrates that on a molar basis, the calcium extraction efficiency remains approximately constant when varying the acetic acid concentration between 0.5 and 2 M, within the range of 21-24 % overall (28 % ± 4 % in the step one, and 16 % ± 6 % in step two). This means that Ca extraction is linearly proportional to acid loading at this range. Hence, mass transfer limitations control leaching extent more so than acidity, given the similar loss of efficiency in step two. The total extent of Ca leaching reached 21 % at 0.5 M, 47 % at 1 M, and 90 % at 2 M.

Looking at selectivity, it is seen that acetic acid also dissolves the magnesium content of GBFS to a significant degree, with its extraction extent slightly surpassing that of calcium. Still, the total amount of Mg extracted is a fraction of the amount of Ca extracted, given the 3.5 times

greater molar content of CaO versus MgO in GBFS. More notable is the extraction of aluminum, which increases significantly at 2 M acetic acid concentration, reaching 38 % total extraction, compared to only 2.1% when using 0.5 M acetic acid. This amount of aluminum loss can potentially have negative implications for the synthesis of zeolitic materials in the hydrothermal stage, and similarly can have implications on the qualities of PCC produced in the carbonation stage; more discussion on this in Sections 3.2 and 3.3. Silicon leaching is more contained, but also increases proportionally to acetic acid concentration, reaching 7.6 % extraction at 2 M.

Based on these results, it appears, from the point of view of selectivity, useful to divide the extraction stage in multiple steps, thus reducing acidity and improving selectivity for Ca and Mg versus Al and Si. On the other hand, this approach increases processing complexity and post-processing acetic acid regeneration demand (i.e. more acetic acid is used and neutralized per unit of PCC produced). In the next sections, the impacts of the different extraction extents and selectivities achieved with varying acid concentrations on the other two processing stages will be elucidated. This shall allow better assessment whether extraction extent/specific acid consumption or selectivity is most important to achieve the valorization and zero-waste goals of the conceptualized process.

3.2. Carbonation results

The production of precipitated calcium carbonates (PCC) was performed by subjecting the leachates from the extraction stage to carbonation treatment. Besides using leachates produced using varying concentration of acetic acid, three additional parameters were varied for investigation of their effect on PCC properties: process temperature (90 or 120 °C), CO_2 partial pressure (6 or 40 bar) and neutralization additive ($NaHCO_3$ or NaOH). The lower process temperature was matched with the lower CO_2 partial pressure, and conversely the higher process temperature was combined with higher CO_2 partial pressure, to equilibrate the countering effects of these parameters on CO_2 solubility [22]. These combinations of temperature and pressure result in higher CO_2 solubility than that of 1 atm,CO_2 at ambient temperature, and are intended to promote rapid carbonation. The variation of these process parameters was done to assess their effect on the precipitation selectivity for calcium in the formation of PCC, and on the properties of the product. The choice of neutralization additives was made to compare a compound

8

produced during CO_2 capture, namely $NaHCO_3$ [23], with a virgin chemical, NaOH. The utilization of the former is interesting from the point of view of reduction of CO_2 capture costs. Since it contains CO_2, its use would reduce the amount of gaseous CO_2 needed for the process. This would in turn reduce costs associated with regeneration of the sorbent for the production of gaseous CO_2.

The precipitation extent of calcium upon carbonation was nearly complete at all tested conditions (Figure 4); 96-99 %. This confirms that the pH neutralization effect of the additives effectively buffered the release of acetic acid. In comparison, Kakizawa et al. [24], who first proposed the use of acetic acid in the production of PCC, did not surpass ~20% calcium precipitation without the use of a neutralizer. The amount of magnesium precipitation grew substantially as the acetic acid concentration increased; Mg precipitation was in the range of 20-23 % at 0.5 M, increasing to 67-84 % at 1 M, and to 88-98 % at 2 M. WDXRF analysis of the precipitates (Table 1) confirms these results.

At higher acetic acid concentrations, larger amounts (equimolar to acetic acid) of alkaline additive were used; incomplete additive neutralization at high concentrations may have led to increased basicity during carbonation, promoting Mg precipitation. Given Mg appears to precipitate less readily, and that it likely is present as an acetate in the pre-carbonation leachate, it may be possible to limit its precipitation by reducing the concentration of added alkali neutralizer to the concentration of calcium acetate in the leachate, rather than total acetate concentration. Also, it is evident from Figure 4 that magnesium precipitation increases at the higher combination of temperature and pressure used; an average precipitation extent improvement of 10 %. The precipitation of calcium, however, was weakly affected by increasing the processing intensity (average precipitation improvement of 1 %). Thus, lowering the carbonation intensity appears to concurrently improve PCC purity and reduce processing energy demand, and would be advisable for industrial implementation.

Similar to Ca, Al precipitation extent was also essentially independent of carbonation conditions; its content in the PCC's ranged from 0.5 to 3.2 wt% (Table 1). Si precipitation, on the other hand, behaved more similarly to Mg precipitation; its content in the PCC's ranged from 0.9 to 3.5 wt% (Table 1). Other impurities detected by WDXRF included Fe (0.2-0.5 wt%), Mn (~0.3 wt%), Sr (avg. 490 ppm), Ti (avg. 450 ppm) and S (avg. 220 ppm). The last two lines of Table 1 totalizes the carbonate content of the precipitates (86.0-95.9 wt%), and the impurity

9

content (4.1-14.0 wt%). Optimization of the additive to acetic acid ratio, as previously discussed, may also be a potential route to minimize Al and Si precipitation. Another approach is to adjust the pH value of the acetate solution towards a neutral value before it is carbonated in order to induce the precipitation of impurities; for example, Al may precipitate in the form of gibbsite $(Al(OH)_3)$ or diaspore $(AlO(OH))$ at pH values above 4.6 and 4.3, respectively (Visual MINTEQ ver. 3.1 beta, 25 °C, 0.1 molal total metal, 10^{-4} molal soluble). The effect of chemical composition (and the speciation of the contaminants) on optical properties of the PCC's, important for certain commercial applications as highlighted by the work of Bunkholt and Kleiv [21] on pyrrhotite ($Fe_{(1-x)}S$, x = 0-0.17), pyrite (FeS_2) and magnetite (Fe_3O_4) contaminants in PCC, should also be investigated.

The carbonation processing conditions also had a significant influence on mineralogical and morphological properties of the carbonation precipitates. X-ray diffractograms (Figure 5) indicate that the major mineral phases vary among three polymorphs of calcium carbonate ($CaCO_3$), namely calcite, vaterite and aragonite, and magnesium-substituted (magnesian) calcite (approximate formula $Ca_{0.85}Mg_{0.15}CO_3$). These differences are clearly visible in SEM images of the precipitates (Figure 6); rhombohedral calcite crystals (Figures 6a, 6c, 6e and 6f), acicular aragonite crystals (Figure 6b), and spherical vaterite crystals (Figure 6d) can be identified.

By Rietveld refinement it is also possible to infer the presence of other carbonate phases (Table 2), present in amounts ranging from 2 to 10 wt%. These include hydrated calcium and magnesium carbonates, anhydrous magnesium carbonate, and calcium-magnesium carbonates: monohydrocalcite ($CaCO_3 \cdot H_2O$), hydromagnesite ($Mg_5(CO_3)_4(OH)_2 \cdot 4H_2O$), nesquehonite ($Mg(HCO_3)(OH) \cdot 2H_2O$), magnesite ($MgCO_3$), dolomite ($CaMg(CO_3)_2$), and huntite ($Mg_3Ca(CO_3)_4$). The results in Table 2 also suggest that more varied carbonate phases form at the milder carbonation condition, with exception of the 0.5 M acetic acid sample. In the case of the 1 M solution, significant quantities of magnesian calcite and vaterite formed, while in the case of the 2 M solution aragonite was the dominant phase. More dedicated research is needed to understand what effects are causing these mineralogical variations, which can include the presence of impurities promoting or hindering crystal growth of certain phases, and the pH during carbonation which is a function of temperature, CO_2 partial pressure, acetate and neutralizer concentrations.

In view of valorization, it appears possible to control the process parameters to deliver desirable PCC characteristics for particular applications of interest. Another property that is important for the valorization of product is the average particle size and the size distribution. These parameters for the PCC's produced in this study are presented in Figure 7. Applications of PCC including filler and pigment require small and tight distributions [25]. The current products partially meet these requirements, with most samples having a top cut-off particle size of roughly 60 μm, and an average particle size below ~20 μm. Seeing as how the experiments performed herein did not aim at controlling particle size, it should be possible to further optimize these properties by tuning processing parameters such as carbonation time, mixing rate, filtration under pressure, Ostwald ripening, among other approaches used in commercial production of PCC's from pure resources.

3.3. Hydrothermal conversion results

The residues from acetic acid extraction were subjected to hydrothermal conversion to convert the amorphous solids (Figure 2) into crystalline materials with zeolitic composition and properties. Three residues were utilized, originating from experiments performed with varying acetic acid concentrations, namely 0.5, 1.0 and 2.0 M. The main characteristics that affect the final product from this processing state are the calcium content (higher in those residues exposed to lower acetic acid concentrations) and the aluminum content (lower in those residues exposed to higher acetic acid concentrations) of the residues. Furthermore, the effect of varying the concentration of NaOH during hydrothermal conversion, between 1 and 3 M, was also investigated. The addition of alkali in this stage has two objectives: (i) to solubilize the silica content of the residue by increasing the OH^- concentration of the solution, thus shifting the chemical equilibrium from poorly soluble silicic acid to highly soluble sodium silicate [26], and (ii) to participate in the synthesis of zeolitic products, several of which contain sodium in their structure [27].

The mineralogical properties of the converted materials where characterized by X-ray diffraction; diffractograms are shown in Figure 8 and Rietveld refinement quantification results are presented in Table 3. The converted extraction residues display diffraction peaks corresponding to four main crystalline phases: tobermorite ($Ca_5(OH)_2Si_6O_{16}.4H_2O$), sodalite

11

($Na_8Al_6Si_6O_{24}Cl_2$), lazurite ($Na_6Ca_2(Al_6Si_6O_{24})(SO_4,S_3,S_2,Cl,OH)_2$), and analcime ($NaAlSi_2O_6 \cdot H_2O$).

The tobermorite phase detected is due to the incomplete removal of calcium in the extraction stage, as its occurrence is greater in samples prepared from residues treated with lower acetic acid concentrations (i.e. 0.5 M and 1 M). The formation of tobermorite, a component found in certain hydrated cements and autoclaved concretes [28], and the possible formation of other forms of poorly crystalline calcium-silicate-hydrates (undetectable by X-ray diffraction), resulted in significant hardening of these dried samples, which required milling prior to analyses.

When sufficient calcium was extracted, laruzite and sodalite appeared in significant quantities. These two mineral phases belong to the sodalite group of minerals and are considered semi-condensed zeolites, having properties that relate both to true zeolites and to complex oxides [29]. These characteristics may impart attractive application potential, for example, in terms of ion exchange and magnetic, optical or electronic effects. One particular property of these minerals is their deep blue color, which was visualized in the dried samples. The color was more intense prior to milling, likely as the crystals were larger.

Analcime formation was possible when the concentration of sodium hydroxide in the hydrothermal stage was reduced to 0.5 and 1 M. The sharp peaks of analcime dominate the diffractograms of the two materials containing this mineral (Figure 8). Analcime is a zeolitic material with irregular channels that is rarely found in nature [30]. Its recent application in, for example, selective adsorption reactions and heterogeneous catalysis [31], has stimulated the search for novel synthesis routes from different local sources of silica and alumina. In the analcime-rich materials prepared in the present study, the formation of tobermorite was significantly suppressed, likely as a consequence of the lower basicity hindering the precipitation of calcium.

The analcime-rich materials attained unique spherical particle morphology (Figure 9, subfigures a and b), with the spheres being smaller in the case of 0.5 M NaOH use in the hydrothermal conversion stage (~3 μm diameter compared to ~10 μm in the case of 1 M NaOH). Because of the absence of significant amounts of tobermorite, the material was powdery and therefore did not undergo milling. The morphology of the sodalite/lazurite-rich materials differs, as crystalline features cannot be easily distinguished (Figure 9, subfigures c and d). Still, EDX analysis captured the chemical signature typical of zeolitic sodium aluminum silicates (Figure

12

10). For the material originating from 0.5 M acetic acid extraction and subsequent hydrothermal conversion with 3 M NaOH, large flakes of tobermorite crystals, similar to those observed by Jackson et al. [28], are seen covering particles that resemble the original slag particles (Figure 9e).

The preferable formation of analcime over sodalite at lower bacisity has been highlighted by the work of Querol et al. [27] on the hydrothermal conversion of coal fly ashes. However, unlike that study, Na-P1 zeolite formation was not detected in the present samples. Murakami et al. [17] was able to obtain Na-P1 and Zeolite A at a lower synthesis temperature of 70 °C, compared to 150 °C used in the present study. Azizi et al. [31] observed formation of analcime at a crystallization temperature of 110 °C or above; at lower temperatures (85-110 °C) zeolites P and Y were obtained. Lower temperatures are likely beneficial to the formation of more hydrated compounds, such as Na-P1 and zeolite A, which contain 12 to 27 waters of hydration, compared to none or one in the case of sodalite minerals and analcime, respectively.

The preferable formation of analcime from the 2 M acetic acid residue in the present study may also be a result of the rather high Si:Al molar ratio in the extraction residue of 4.8 (76.9 wt% SiO_2, 13.5 wt% Al_2O_3, determined by WDXRF), which is closer to the ratio found in analcime, namely 2, than to that found in Na-P1 or zeolite A, namely 1. Sodalite and lazurite, which formed in large amounts from 1 M acetic acid residues, also have Si:Al ratio of 1, but since co-formed tobermorite also contains 6 moles of Si per mole, the consumption of Si becomes about double that of Al.

Wałek et al. [32] suggest that higher temperatures can be used during the initial stage of the hydrothermal reaction to promote silica dissolution, while lower temperatures can be used in the later stage to promote the formation of zeolitic materials possessing high pore volumes and thus improved cation exchange capacity (CEC), ideal for certain applications including sorbents [11]. Indeed, the BET specific surface area of the materials herein prepared, determined by N_2 adsorption and attributable primarily to the presence of micropores, increased moderately after hydrothermal synthesis, from an initial 3.7 m^2/g for milled GBFS to 8.3-19.5 m^2/g for the converted residues. Thus optimization of the hydrothermal conversion stage has the potential to lead to higher value products for commercially existing or newly developed applications.

13

4. Conclusions

This work has investigated the possibility of transforming blast furnace slag (BFS) into two valuable products within the same process: precipitated calcium carbonate (PCC) and zeolitic materials. To achieve this goal symbiotically, and with minimal solid waste generation, an integrated process was developed. In the first stage, calcium is to be extracted selectively from BFS by leaching with organic acids, generating a calcium-rich solution, and a solid residue depleted in calcium. The leachate solution from this stage is then to be carbonated in a second stage to induce the precipitation of (primarily) calcium carbonate. In parallel, the solid residue from the first-stage extraction is to undergo hydrothermal conversion in highly alkaline solution to induce the dissolution/precipitation mechanism that leads to the formation of micro- and meso-porous zeolitic materials. Experiments were performed to study the interrelationships between these three stages, and how processing conditions can be tuned to maximize the valorization potential of the products.

Acetic acid was trialed for the first stage leaching. Its use satisfactorily limited the leaching of aluminum, required for the subsequent synthesis of zeolites, while enabling, at high concentrations, nearly complete calcium extraction. Extensive calcium leaching was found to be more important than selectivity in view of the products formed in the hydrothermal conversion stage. If further optimization on the extraction process is to be performed (i.e. with different leaching agents or processing conditions), such work should focus on maintaining high calcium extraction, while attempting to minimize even further the leaching of the other components.

Carbonation of the acetic acid leachate resulted in the production of the desired PCC product, with total calcium precipitation and partial magnesium precipitation. Small quantities of aluminum and silicon were found to end up as contaminants of the precipitate. Purification of the leachate prior to carbonation appears to be necessary to improve product qualities, and deserves further research and development. This could be done either by selective removal of impurities prior to carbonation, using chemical or physicochemical methods, and/or by attenuating the quantity of neutralizer added to the carbonation process, coupled to precipitate separation at processing conditions (i.e. prior to cooling and pressure release).

The mineralogy and particle morphology of the PCC product was seen to vary depending on carbonation conditions (temperature and pressure), ranging from rhombohedral calcite, to

14

acicular aragonite, to spherical vaterite. The particle size (average and distribution) of the PCC's are close to the required properties for application as fillers and pigments, though slightly on the large side. This suggests that optimization of the process to maximize the product's valorization potential is possible.

In the hydrothermal stage, the solid residue, containing primarily silica and aluminum oxide, was converted successfully into zeolitic products. These products varied depending on the level of calcium extraction of the first stage (a function of the organic acid concentration utilized) and the processing conditions used in the hydrothermal stage (in this study NaOH concentration variation was studied, but temperature and duration, as known from literature [11, 14, 27], can also be used to control product properties). Tobermorite, a less desirable product, formed when the calcium content of the residue was rather high. Sodalite and lazurite, blue-colored semi-condensed zeolites, formed when the calcium content was reduced. This further emphasizes the importance of high efficiency in the extraction stage. Lowering the NaOH concentration from 3 to 1 or 0.5 molar resulted in the formation of analcime, a zeolitic material with attractive valorization potential. As in the case of PCC production, the results herein reported suggest that zeolitic product properties can be tuned for intended applications by operating at particular process conditions.

With the proof-of-concept confirmed, further research and development on the proposed two-way valorization process is warranted to find the conditions that maximize economic value, and thus that present the best opportunity to turn mineral carbonation into a sustainable and zero-waste solution for CO_2 sequestration.

Acknowledgements

References

[1]   S. Teir, S. Eloneva, C.-J. Fogelholm, R. Zevenhoven, Dissolution of steelmaking slags in acetic acid for precipitated calcium carbonate production, Energy 32 (2007) 528-539.

[2]   S. Eloneva, S. Teir, J. Salminen, C.-J. Fogelholm, R. Zevenhoven, Fixation of CO_2 by carbonating calcium derived from blast furnace slag, Energy 33 (2008) 1461-1467.

[3]   Y. Sun, M.-S. Yao, J.-P. Zhang, G. Yang, Indirect CO_2 mineral sequestration by steelmaking slag with NH_4Cl as leaching solution, Chem. Eng. J. 173 (2011) 437-445.

[4]   W. Bao, H. Li, Synthesis of aragonite superstructure from steelmaking slag via indirect CO_2 mineral sequestration, World Academy of Science, Engineering and Technology 65 (2012) 1036-1042.

[5]   S. Eloneva, A. Said, C.-J. Fogelholm, R. Zevenhoven, Preliminary assessment of a method utilizing carbon dioxide and steelmaking slags to produce precipitated calcium carbonate, Appl. Energy 90 (2012) 329-334.

[6]   A. Said, H.-P. Mattila, M. Järvinen, R. Zevenhoven, Production of precipitated calcium carbonate (PCC) from steelmaking slag for fixation of CO_2, Appl. Energy 112 (2013) 765-771.

[7]   S. Eloneva, E.-M. Puheloinen, J. Kanerva, A. Ekroos, R. Zevenhoven, C.-J. Fogelholm, Co-utilisation of CO_2 and steelmaking slags for production of pure $CaCO_3$ – legislative issues, J. Cleaner Prod. 18 (2010) 1833-1839.

[8]   R.M. Santos, D. Ling, A. Sarvaramini, M. Guo, J. Elsen, F. Larachi, G. Beaudoin, B. Blanpain, T. Van Gerven, Stabilization of basic oxygen furnace slag by hot-stage carbonation treatment, Chem. Eng. J. 203 (2012) 239-250.

[9]   H.G. van Oss, Slag—Iron and Steel, in: 2011 Minerals Yearbook, U.S. Geological Survey, 2011.

[10]   R. Siddique, M.I. Khan, Supplementary Cementing Materials, Springer, Berlin, 2011.

[11] Y.W. Chiang, K. Ghyselbrecht, R.M. Santos, B. Meesschaert, J.A. Martens, Synthesis of zeolitic-type adsorbent material from municipal solid waste incinerator bottom ash and its application in heavy metal adsorption, Cat. Today 190 (2012) 23-30.

[12] CCA Europe, Mineral Applications, The European Calcium Carbonate Association. http://www.cca-europe.eu/mineral-applications.html (date accessed 11.02.2014).

[13] A. Shoumkova, Zeolites for water and wastewater treatment: An overview, 2011 Research Bulletin of the Australian Institute of High Energetic Materials 2 (2011) 10-70.

[14] Y. Sugano, R. Sahara, T. Murakami, T. Narushima, Y. Iguchi, C. Ouchi, Hydrothermal synthesis of zeolite A using blast furnace slag, ISIJ Int. 45 (2005) 937-945.

[15] Y. Kuwahara, T. Ohmichi, T. Kamegawa, K. Mori, H. Yamashita, A novel conversion process for waste slag: synthesis of a hydrotalcite-like compound and zeolite from blast furnace slag and evaluation of adsorption capacities, J. Mater. Chem. 20 (2010) 5052-5062.

[16] E.R. Bobicki, Q. Liu, Z. Xu, H. Zeng, Carbon capture and storage using alkaline industrial wastes, Prog. Energy Combust. Sci. 38 (2012) 302-320.

[17] T. Murakami, Y. Sugano, T. Narushima, Y. Iguchi, C. Ouchi, Recovery of calcium from BF slag and synthesis of zeolite A using its residue, ISIJ Int. 51 (2011) 901-905.

[18] E. Bingham and B. Cohrssen, Patty's Toxicology, John Wiley & Sons, Hoboken, sixth ed., vol. 3, p. 472.

[19] R. Snellings, L. Machiels, G. Mertens, J. Elsen, Rietveld refinement strategy for quantitative phase analysis of partially amorphous zeolitized tuffaceous rocks, Geologica Belgica 13 (2010) 183-196.

[20] M. Back, M. Bauer, H. Stanjek, S. Peiffer, Sequestration of CO_2 after reaction with alkaline earth metal oxides CaO and MgO, Appl. Geochem. 26 (2011) 1097-1107.

[21] I. Bunkholt, R.A. Kleiv, The colouring effect of pyrrhotite and pyrite on micronised calcium carbonate slurries for the paper industry, Min. Eng. 52 (2013) 104-110.

[22] R.M. Santos, J. Van Bouwel, E. Vandevelde, G. Mertens, J. Elsen, T. Van Gerven, Accelerated mineral carbonation of stainless steel slags for CO_2 storage and waste valorization: effect of process parameters on geochemical properties, Int. J. Greenhouse Gas Control 17 (2013) 32-45.

[23] M. Yoo, S.-J. Han, J.-H. Wee, Carbon dioxide capture capacity of sodium hydroxide aqueous solution, J. Environ. Manage. 114 (2013) 512-519.

[24] M. Kakizawa, A. Yamasaki, Y. Yanagisawa, A new CO_2 disposal process via artificial weathering of calcium silicate accelerated by acetic acid, Energy 26 (2001) 341-354.

[25] R.W. Hagemeyer, Calcium Carbonate, in: R.W. Hagermeyer (Ed.), Pigments for Paper, TAPPI Press, Atlanta, 1984, pp. 74-81.

[26] R. Helmuth, D. Stark, S. Diamond, M. Moranville-Regourd, Alkali-Silica Reactivity: An Overview of Research, Strategic Highway Research Program Report SHRP-C-342, National Research Council, Washington D.C., 1993.

[27] X. Querol, J.C. Umaña, F. Plana, A. Alastuey, A. Lopez-Soler, A. Medinaceli, A. Valero, M.J. Domingo, E. Garcia-Rojo, Synthesis of zeolites from fly ash at pilot plant scale. Examples of potential applications, Fuel 80 (2001) 857-865.

[28] M.D. Jackson, J. Moon, E. Gotti, R. Taylor, S.R. Chae, M. Kunz, A.-H. Emwas, C. Meral, P. Guttmann, P. Levitz, H.-R. Wenk, P.J.M. Monteiro, Material and elastic properties of Al-tobermorite in ancient Roman seawater concrete, J. Am. Ceram. Soc. 96 (2013) 2598-2606.

[29] M.T. Weller, Where zeolites and oxides merge: semi-condensed tetrahedral frameworks, J. Chem. Soc., Dalton Trans. 2000 (2000) 4227-4240.

[30]   A.Y. Atta, B.Y. Jibril, B.O. Aderemi, S.S. Adefila, Preparation of analcime from local kaolin and rice husk ash, Appl. Clay Sci. 61 (2012) 8-13.

[31]   S.N. Azizi, A.A. Daghigh, M. Abrishamkar, Phase Transformation of Zeolite P to Y and analcime zeolites due to changing the time and temperature, Journal of Spectroscopy 2013 (2013) 428216.

[32]   T.T. Wałek, F. Saito and Q. Zhang, The effect of low solid/liquid ratio on hydrothermal synthesis of zeolites from fly ash, Fuel 87 (2008) 3194-3199.

List of Figures

Fig. 1. Conceptualized flowsheet of two-way valorization of blast furnace slag.

Fig. 2. X-ray diffractograms of milled granulated blast furnace slag (red) and residue from acetic acid extraction stage (black).

Fig. 3. Results of organic acid extraction (first and second stages, and total) of Al, Ca, Mg and Si from milled GBFS, at 30 °C and for 60 minutes, using varying concentrations of acetic acid (0.5 –2.0 M).

Fig. 4. Extent of Ca and Mg precipitation from extraction leachates after carbonation.

Fig. 5. X-ray diffractograms of post-carbonation precipitates from acetic acid leachates; major mineral phases ($\geq$ 10 wt%) indicated.

Fig. 6. Morphology of post-carbonation precipitates from acetic acid leachates, visualized by SEM.

Fig. 7. Volume-based particle size distribution and mean particle diameter (D[4,3]) of post-carbonation precipitates from acid acid leachates, determined by laser diffraction.

Fig. 8. X-ray diffractograms of acetic acid residues after hydrothermal conversion; zeolitic phases indicated; intensities of analcime-containing materials are scaled-down by factor of four.

Fig. 9. Morphology of acetic acid residues after hydrothermal conversion, visualized by SEM.

Fig. 10. Chemical analysis by energy dispersive X-rays (EDX) of zeolitic material shown in Figure 9d (central image).

20

List of Tables

Table 1

wt%	0.5 M acetic acid leachate		1 M acetic acid leachate		2 M acetic acid leachate	
	90°C, 6 bar $NaHCO_3$	120°C, 40 bar NaOH	90°C, 6 bar $NaHCO_3$	120°C, 40 bar NaOH	90°C, 6 bar NaOH	120°C, 40 bar NaOH
Ca	35.7%	35.3%	31.8%	30.8%	27.5%	27.4%
Mg	1.6%	2.2%	3.8%	4.6%	5.1%	5.0%
Si	1.3%	0.9%	1.6%	1.5%	3.4%	3.5%
Al	0.7%	0.5%	1.8%	1.7%	3.1%	3.2%
Fe	0.5%	0.5%	0.2%	0.2%	0.2%	0.2%
Mn	0.3%	0.3%	0.3%	0.3%	0.3%	0.3%
Carbonates	94.7%	95.9%	92.5%	93.0%	86.3%	86.0%
Impurities	5.3%	4.1%	7.5%	7.0%	13.7%	14.0%

Table 2

| Mineral phase | 0.5M acetic acid leachate | | 1M acetic acid leachate | | 2M acetic acid leachate | |
	90°C, 6 bar NaHCO$_3$	120°C, 40 bar NaOH	90°C, 6 bar NaHCO$_3$	120°C, 40 bar NaOH	90°C, 6 bar NaOH	120°C, 40 bar NaOH
Aragonite	<	<	<	<	64.1	3.8
Calcite	72.9	65.8	25.6	77.9	14.1	63.7
Calcite, magnesian	15.5	13.7	19.9	2.9	4.9	7.8
Dolomite	<	5.5	2.7	3.5	2.2	4.0
Huntite	3.6	3.7	3.2	<	<	10.6
Hydromagnesite	<	<	4.3	<	<	<
Magnesite	<	<	10.0	2.3	<	2.4
Monohydrocalcite	2.6	3.5	<	<	<	<
Nesquehonite	<	<	<	5.5	4.4	<
Vaterite	<	<	30.9	<	2.2	<

< : less than estimated quantification accuracy of ± 2.0 wt%.

Table 3

Extraction:	0.5 M acet.ac.	1 M acet.ac.	2 M acet.ac.	2 M acet.ac.	2 M acet.ac.
Hydrothermal:	3 M NaOH	3 M NaOH	3 M NaOH	1 M NaOH	0.5 M NaOH
Analcime	1.1	6.1	4.5	89.7	93.5
Lazurite	0.0	30.8	32.8	0.2	0.5
Quartz	2.4	3.9	1.6	0.8	1.1
Tobermorite	96.1	43.5	33.0	9.0	5.0
Sodalite	0.4	15.7	28.2	0.3	0.0

Figure 1 color for web

Blast Furnace Slag

Organic Acid

Calcium Extraction

Leachate

CO_2 + NaOH

Carbonation

Precipitated calcium carbonate

Residual solids

Hydrothermal Conversion

Spent NaOH

Zeolitic materials

NaOH

Process route
Integration route

Figure 2 color for web

pre- and post-extraction BFS

pre- and post-extraction BFS

counts

560

0

5   10   20   30   40   50   60

2θ

Figure 3
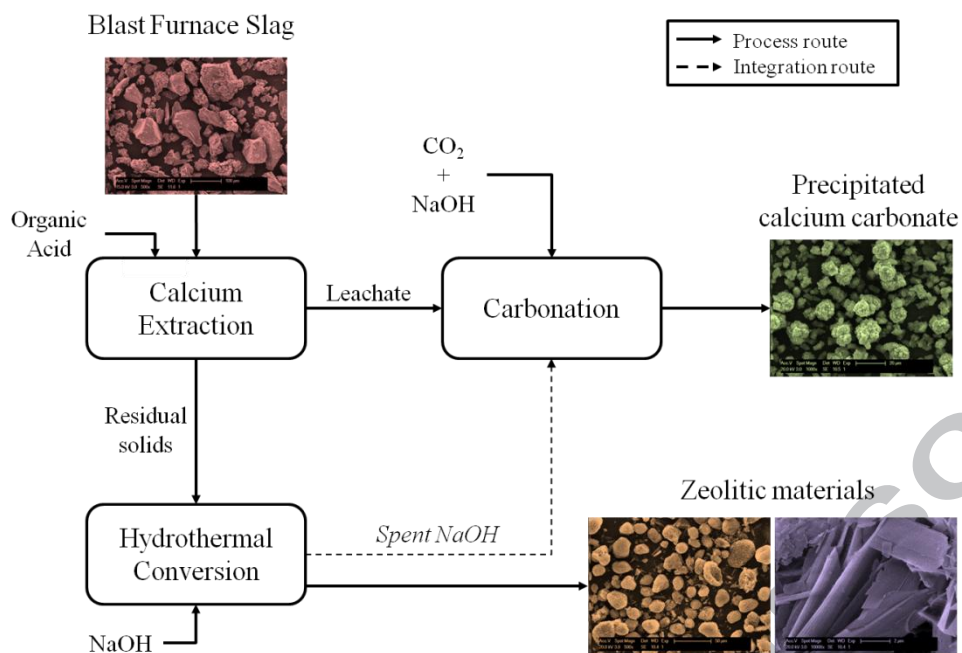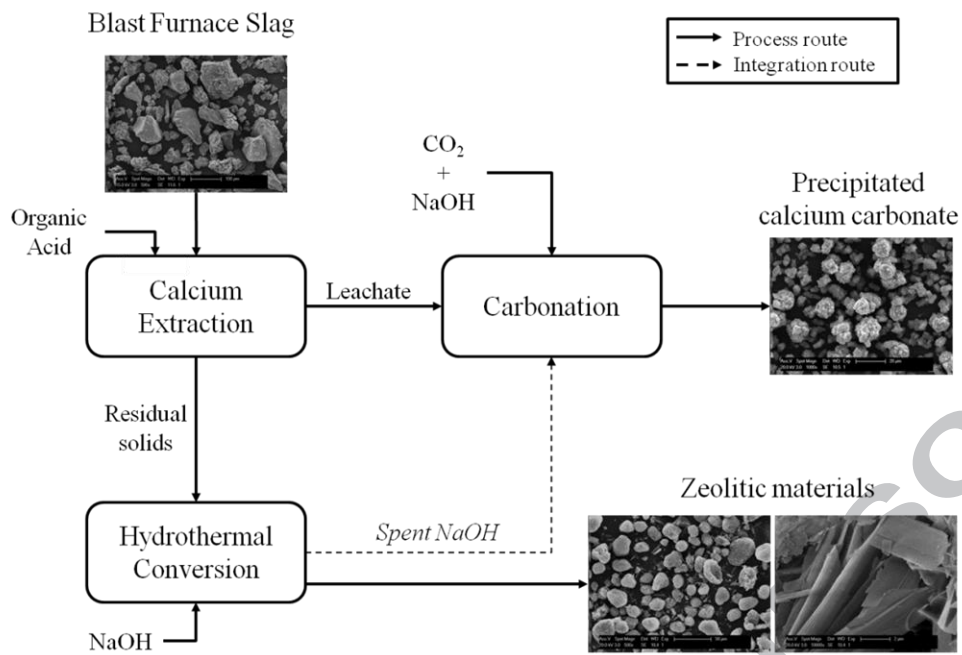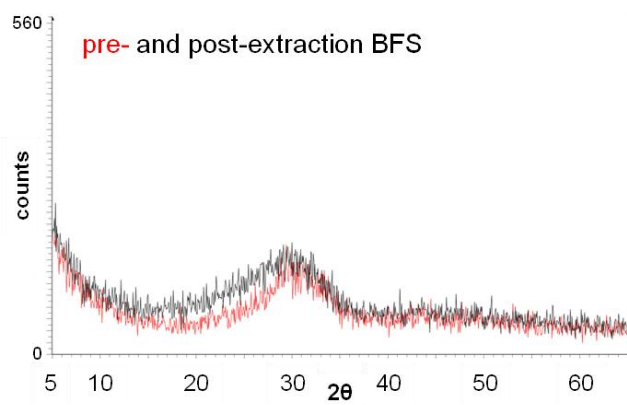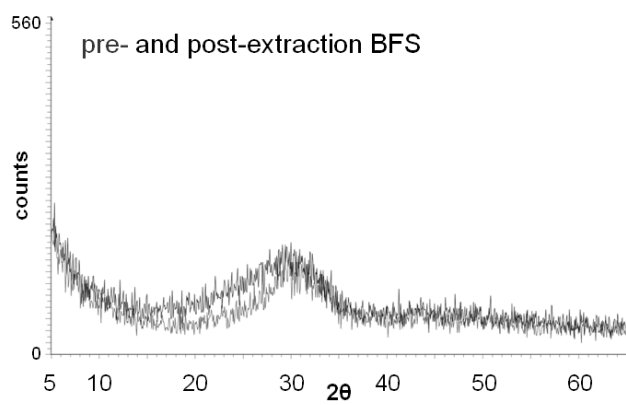
ACCEPTED MANUSCRIPT
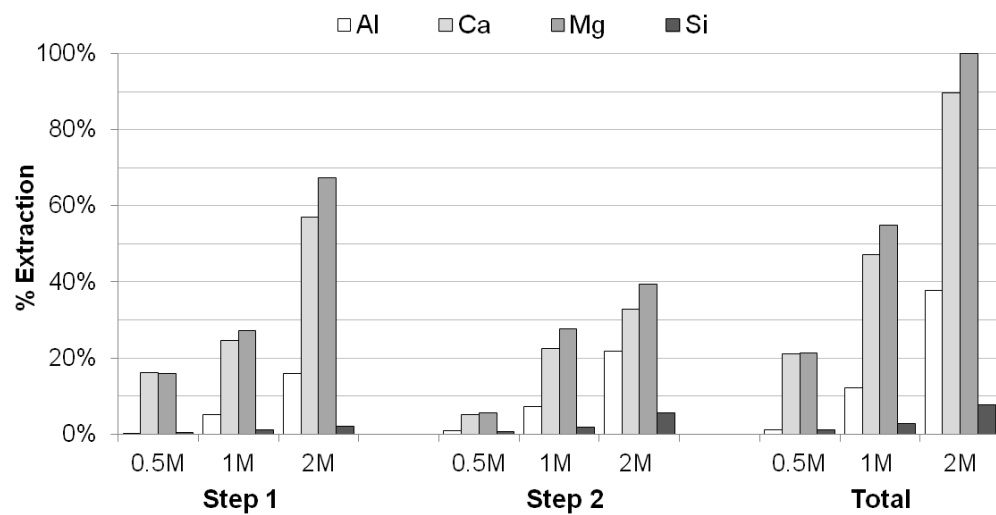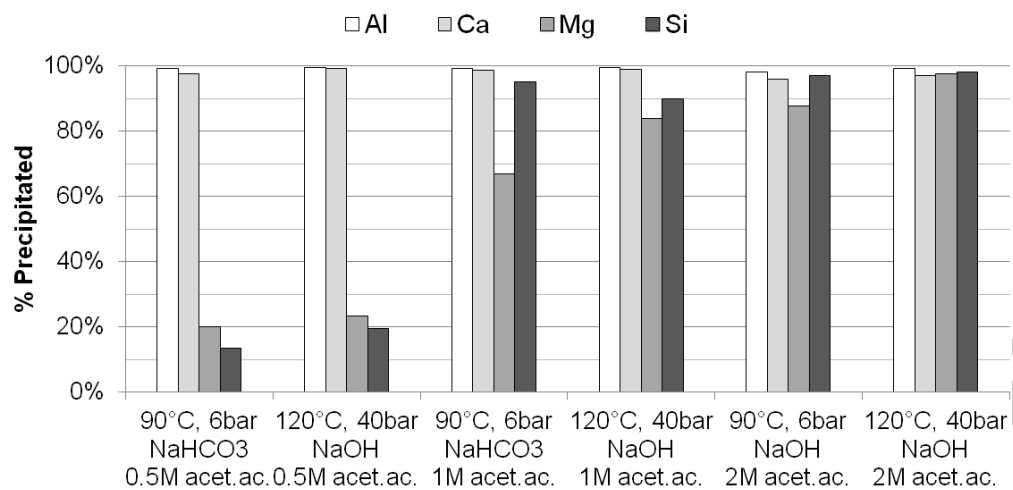
Figure 4

Figure 5

Figure 6
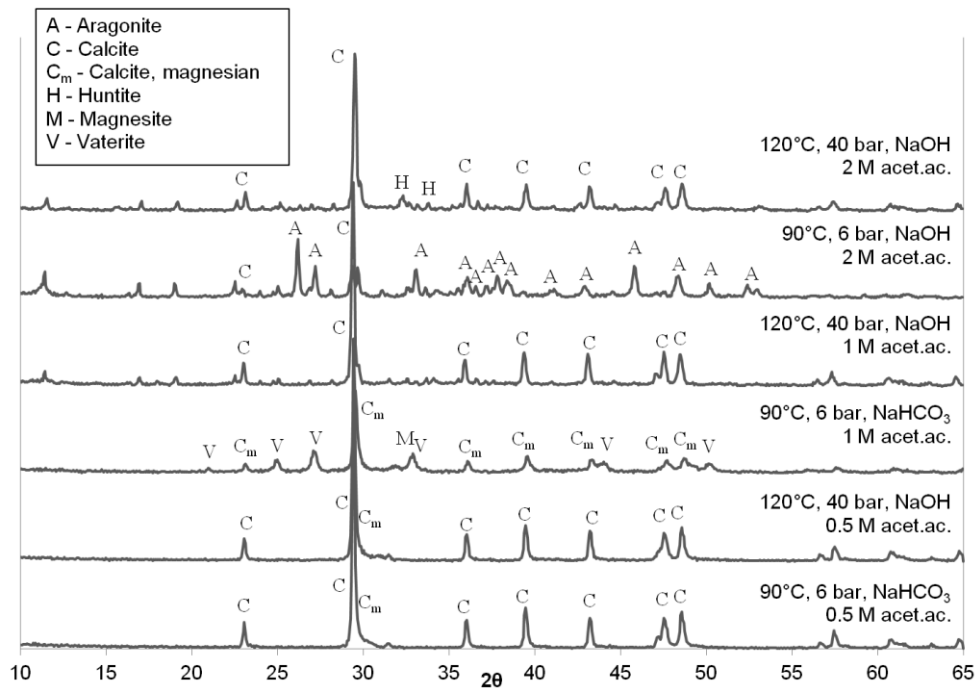
a) 120°C, 40 bar, NaOH
2 M acet.ac.
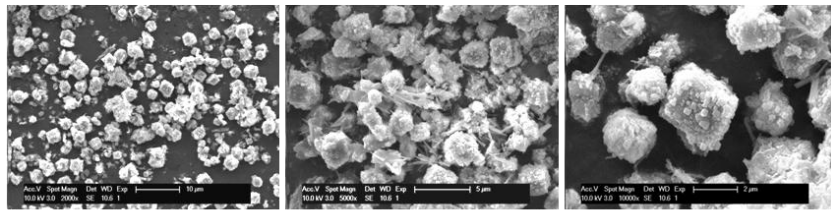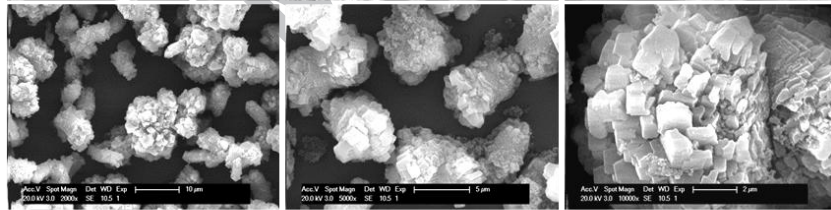
b) 90°C, 6 bar, NaOH
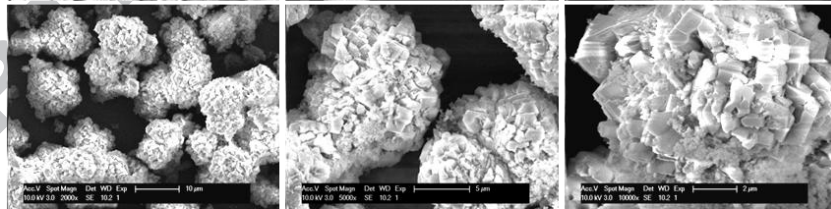2 M acet.ac.
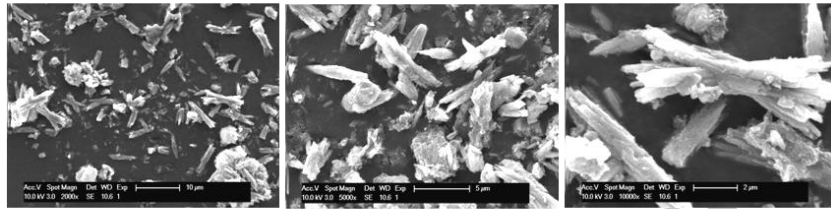
c) 120°C, 40 bar, NaOH
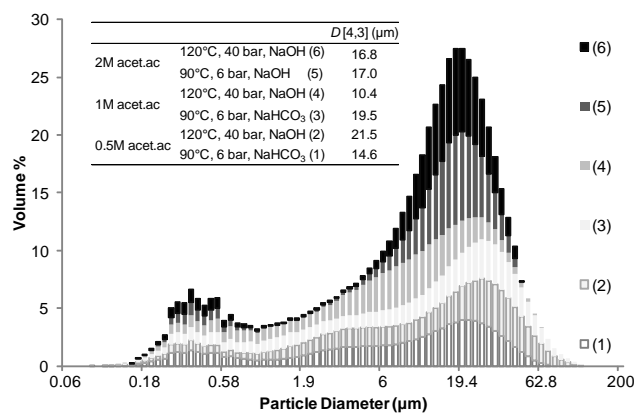1 M acet.ac.
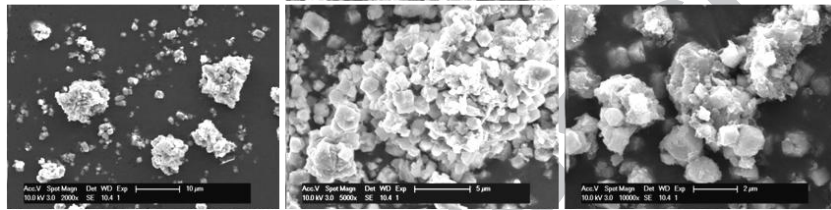
d) 90°C, 6 bar, NaHCO$_3$
1 M acet.ac.
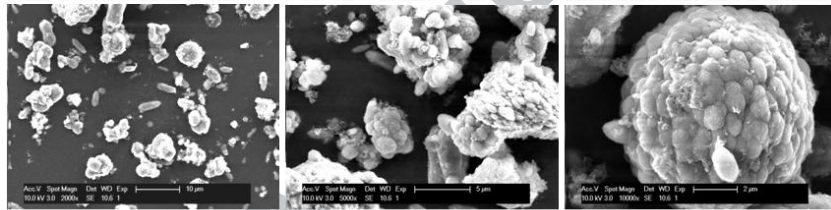
e) 120°C, 40 bar, NaOH
0.5 M acet.ac.

f) 90°C, 6 bar, NaHCO$_3$
0.5 M acet.ac.

Figure 7

		D[4,3] (µm)
2M acet.ac	120°C, 40 bar, NaOH (6)	16.8
	90°C, 6 bar, NaOH (5)	17.0
1M acet.ac	120°C, 40 bar, NaOH (4)	10.4
	90°C, 6 bar, NaHCO$_3$ (3)	19.5
0.5M acet.ac	120°C, 40 bar, NaOH (2)	21.5
	90°C, 6 bar, NaHCO$_3$ (1)	14.6

Particle Diameter (µm)

Figure 8

ACCEPTED MANUSCRIPT

Figure 8

Figure 9

a) 2 M acet.ac.
0.5 M NaOH

b) 2 M acet.ac.
1 M NaOH

c) 2 M acet.ac.
3 M NaOH

d) 1 M acet.ac.
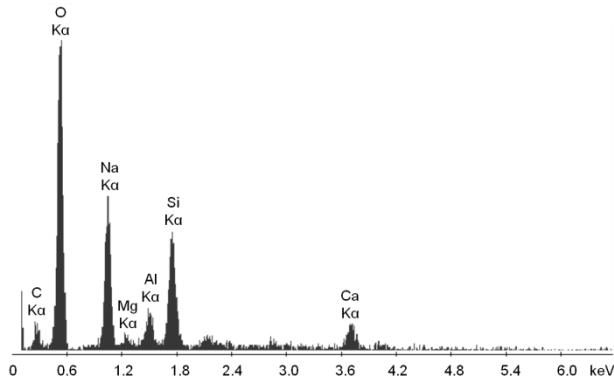3 M NaOH

e) 0.5 M acet.ac.
3 M NaOH

Figure 10
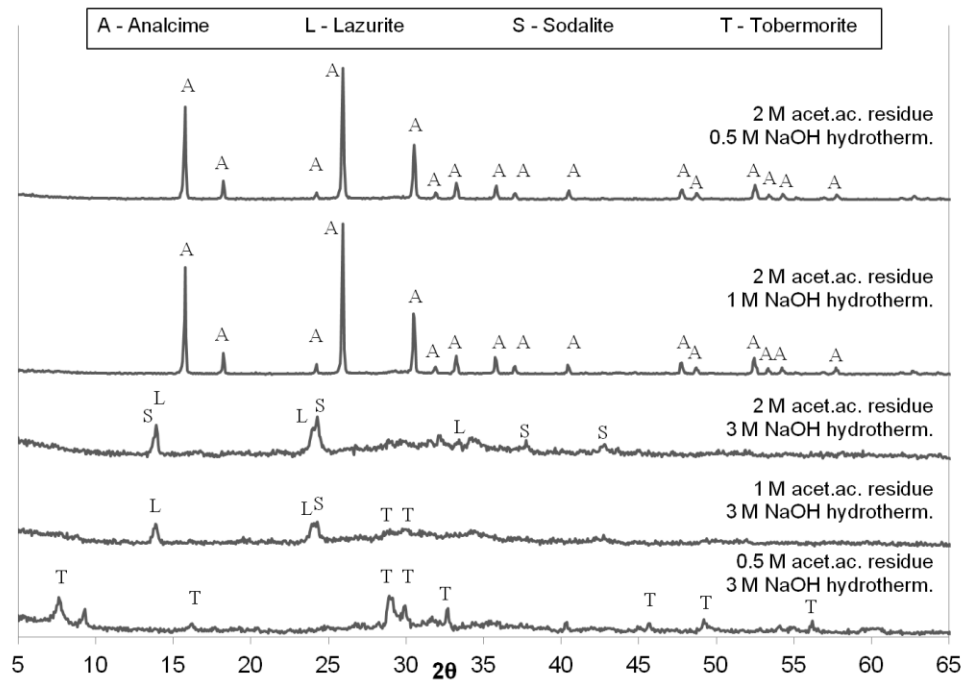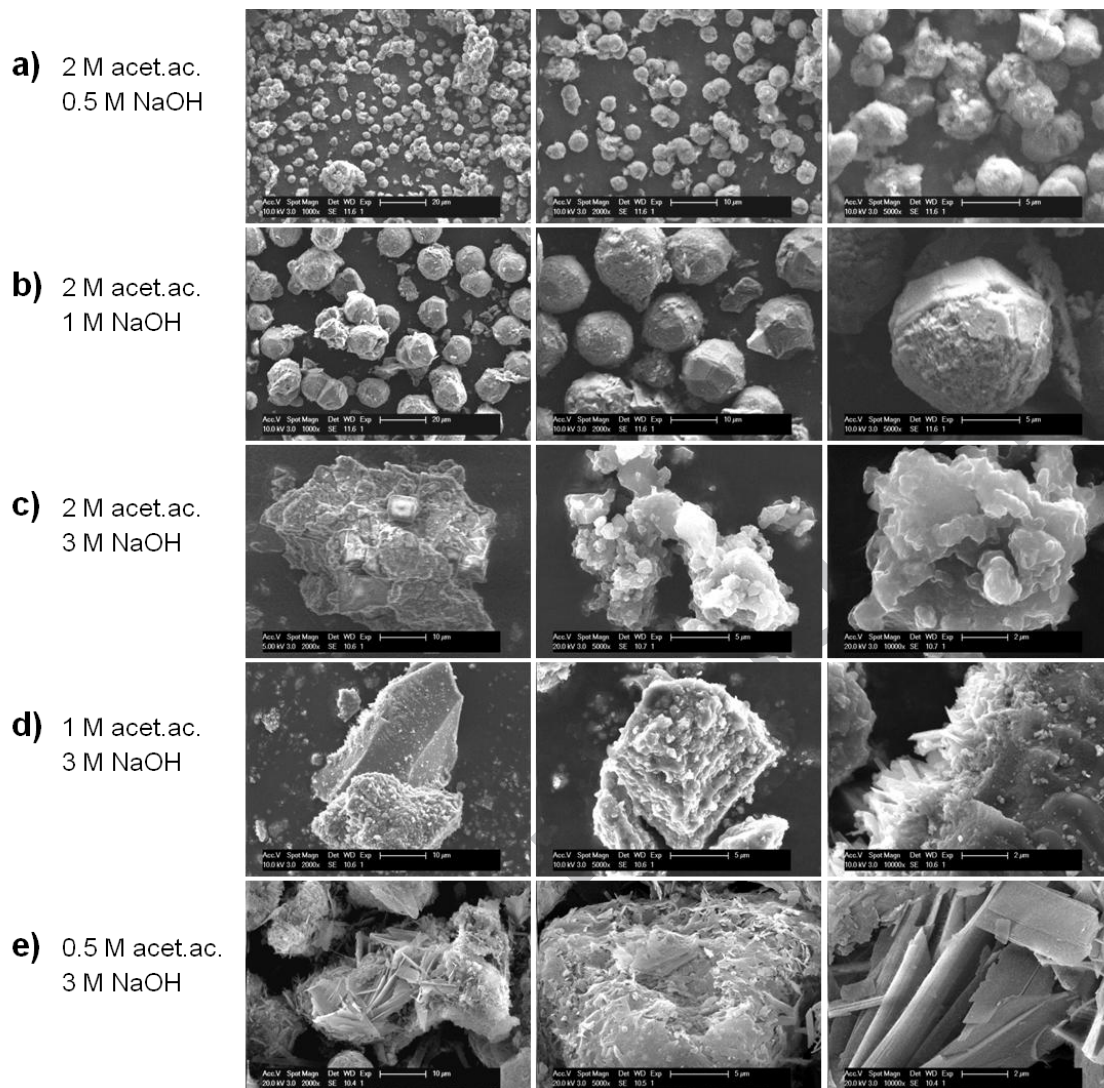
- A symbiotic process is developed to valorize blast furnace slag into two products.
- Carbonation of extracted acetic acid leachate results in the production of PCC.
- Hydrothermal conversion of the extraction residues forms various zeolitic materials.
- Leaching selectivity is a key factor in the valorization potential of both products.